Mechanisms of Ewing sarcoma metastasis : biochemistry and biophysics

Beletkaia, E.

Chapter 3

Differential activation modes of G_α-subunits in chemokine receptor signaling[1]

[1] Elena Beletkaia and Thomas Schmidt

G-proteins are the front-line signal transducing partners of the G-protein coupled receptors (GPCRs). A single GPCR can be activating various G-proteins. It is believed that a specific combination of various G-proteins together with a tight temporal control of their activation is required to ensure faithful and specific signalling through downstream biochemical cascades. Presumably this level of control is facilitated by different modes of coupling of the G-protein to the receptor. Here we investigated the interaction of the chemokine receptor CXCR4 with its corresponding G-proteins. We showed that indeed $G_{\alpha i}$ and $G_{\alpha q}$ exhibit different coupling modes. Variation in the receptor/G-protein interaction was aligned with the subsequent pathways activation and potentially play an important role in regulating CXCR4 specific signalling in cells.

3.1 Introduction

G protein-coupled receptors (GPCRs) are a unique family of membrane receptors that control a wide variety of physiological functions from embryogenesis to immune response. Counting to ∼800 members (Fredriksson et al., 2003), GPCRs do not only share a common seven transmembrane-helix structure, but they also share their front-line signal transduction partners, the G-proteins. The heterotrimeric guanine nucleotide-binding proteins (G-proteins) are encoded by 35 genes in the human genome (Milligan and Kostenis, 2006). The 45 kDa heterotrimers includes the 35 kDa α-subunit and two 8-10 kDa polypeptides defined as the β- and γ-subunits (Milligan and Kostenis, 2006). There are 16 different α-, 5 β-, and 14 γ-subunits (G_α, G_β and G_γ, respectively). The G_α subunits are sub-divided into 4 groups: G_αs which regulates an increase in intracellular cyclic adenosine mono-phosphate (cAMP) concentration, $G_{\alpha i/o}$ which regulates a decrease in cAMP concentration, $G_{\alpha q/11}$ which activates phospholipase C (PLC) subsequently leading to increased cytoplasmic Ca^{2+} levels, and $G_{\alpha 12/13}$ which regulates signalling by the small GTPase Rho. The G_β and G_γ subunits occur presumably as stable heterodimers ($G_{\beta\gamma}$) and are shown to activate multiple pathways, which are partially overlapping with those of the G_α subunits. The precise signal translation from multiple ligands to the specific GPCR is enabled by a peculiar combination of the G-protein subunits activating corresponding specific downstream biochemical response.

The mechanisms by which specificity in receptor/G-protein interaction is controlled are not yet well understood. Knowledge about these mechanisms is highly required for the development of novel drugs leading to more precise targeting, and thus avoiding undesired pharmacological side effects. Extensive research of the past years resulted in the development of two models for this initial receptor/G-proteins interaction (Hein and Bunemann, 2008; Hein et al., 2005). The first, so called 'collision coupling' model, assumes that G-proteins and receptors exist as independent entities in the plasma membrane which, by diffusion, are able to collide initiating the interaction and subsequent activation of the G-protein. The second, so called 'pre-coupling' model, assumes that the receptor/G-protein form a stable complex prior to activation, which on activation is disrupted and the G-protein activated. Activation of the G-protein heterotrimer subsequently leads to the loss of $G_\alpha/G_{\beta\gamma}$ interaction and a split of the trimer into a G_α monomer and a $G_{\beta\gamma}$ heterodimer.

The mode of GPCR and G-protein interaction has been addressed for various systems using fluorescence-based methods. Experiments using fluorescence recovery after photobleaching (FRAP) showed that the α_2A-adrenergic receptor did not form stable complexes with its respective $G_{\alpha i}$ (Qin et al., 2008), while for the μ-opioid receptor such interaction with $G_{\alpha o}$ has been found for resting cells (Qin et al., 2008). Further bioluminescence resonant energy transfer (BRET) and fluorescence resonant energy transfer (FRET) approaches showed that interaction of GPCR and G-proteins is a fast, transient process on a time scale of 30-50 ms, suggesting their plausible pre-coupled state (Lohse et al., 2008). Upon activation the FRET signal decreased rapidly, which would be predicted for the dissociation of a pre-complex (Lohse et al., 2008). However, FRET also revealed that only a small fraction of $G_{\alpha i}$ was pre-coupled to the α_2-adrenoceptor (Hein et al., 2005). Single-molecule fluorescence imaging showed that the G-proteins were pre-coupled to the chemokine cAMP-receptor 1 (cAR1) in Dictyostelium discoideum (van Hemert et al., 2010). Hence, different studies provide support for both models, suggesting that the coupling mode of GPCRs and G proteins might be not universal. It seems tempting to speculate that the differential mode of operation for GPCR/G-protein coupling could be an additional mechanism for spatial and temporal signal propagation control in cells.

An interesting GPCR to study with respect to its coupling mode is the chemokine receptor CXCR4. CXCR4 activates four different G_α subunits (Rubin, 2008), with a major role for $G_{\alpha i}$ and $G_{\alpha q}$ (Teicher and Fricker, 2010). We have shown in a prior study that the mobility of CXCR4 in the plasma membrane reflected its interaction with the respective G-protein. The interaction with $G_{\alpha i}$ was essential for receptor immobilization, while the $G_{\alpha q}$ signalling was interfering with CXCR4 internalization after stimulation by its specific ligand CXCL12 (Chapter 2 of this thesis). In the current study, we further addressed the question of the mechanism of CXCR4/G-protein interaction and its involvement in receptor signalling in the Ewing sarcoma-derived cell line A673. Our results revealed that receptor coupling to $G_{\alpha i}$ and $G_{\alpha q}$ followed different coupling models. While the $G_{\alpha i}$-subunit obeyed the 'collision coupling' model, the $G_{\alpha q}$-subunit appeared as pre-coupled with the receptor. Our findings suggest that G-protein activation by CXCR4 occurs in a sequential manner: an early response by the pre-coupled $G_{\alpha q}$, followed by a later response by $G_{\alpha i}$. Whether and how this time-dependent dif-

ferentiation in G-proteins activation might lead to further specificity in CXCR4 signalling will have to be explored in the future.

3.2 Materials and Methods

3.2.1 Cell culture and transfection

Ewing sarcoma A673 wt cells and A673 cells stably transfected with the chemokine receptor CXCR4 (A673-CXCR4) were cultured in IMDM cell culture medium (Gibco, USA) supplemented with 10% fetal bovine serum (200 μg/mL; FBS, Gibco, USA) at 37°C and 5% CO_2. For transient transfection with CXCR4, $G_{\alpha i}$-YFP, $G_{\alpha q}$-YFP or YFP-G_β/G_γ 0.5×10^5 A673 cells were plated on 0.35 mm diameter culture dishes (Ibidi, Germany) and allowed to adhere overnight. For the transfection mix 1 μg of respective plasmid DNA was diluted in 93 μL serum-free medium and mixed with 4 μL Turbofect. The mix was vortexed and incubated for 20 minutes. Cells were incubated with 100 μL of the transfection mix for 2 hours, followed by medium change and overnight incubation to allow for protein synthesis. For co-transfection an equal amount of respective DNA was pre-mixed to a final concentration of 1 μg/μL and total weight of 1 μg plasmid DNA and was used in the transfection mixture.

3.2.2 Confocal microscopy

Confocal microscopy was performed using an Axiovert200 microscope (Zeiss, Germany) combined with a spinning disk unit (CSU-X1, Yokogawa, Japan) and an emCCD camera (iXon 897, Andor, UK) (van Hoorn et al., 2014). Imaging was performed using a 100×/NA1.4 objective (Zeiss) at 514 nm (Cobolt) laser illumination. Time-lapse imaging was performed at 1 second time lag. Where indicated, CXCL12 was added to the media to a final concentration of 100 nM present in the media during the time of the entire experiment.

3.2.3 Single-molecule imaging

Single-molecule fluorescent imaging was carried out using a combination of wide-field microscopy with highly-sensitivity CCD (Princeton Instruments, USA) or high-sensitivity CMOS (Orca flash 4.0v2, Hamamatsu,

Japan) camera detection as described in detailed elsewhere (Schmidt et al., 1996). To excite individual YFP molecules illumination with a 514 nm laser set to 2 kW/cm^2 intensity and illumination time of 5 ms was applied. The signal was subsequently detected on the camera for 1000-1500 frames at a frame-rate of 20-40 Hz. Each fluorescence signal was fit to a 2D-Gaussian intensity distribution yielding the G-protein position to $\sigma = 40$ nm accuracy. Subsequently all results were filtered with respect to a previously determined YFP-footprint signal (van Hemert et al., 2010). For those data particle image correlation spectroscopy (PICS) was used to construct the cumulative distribution of square displacement (*cdf*) characterizing the protein's mobility (Semrau and Schmidt, 2007). Data were subsequently fit to an n = 2 or n = 3 fraction model:

$$cdf(r^2, t, n) = 1 - \left(\Sigma_{i=1}^{n} \alpha_i \cdot exp(\frac{-r^2}{MSD_i(t)})\right) \tag{3.1}$$

where r^2 is the squared displacement, α_i are the respective normalized fraction sizes ($\Sigma\alpha_i = 1$) of proteins with characteristic mean square displacement MSD$_i$(t) and lag-time t. For free diffusion the MSD is related to the diffusion constant D as

$$MSD_i = 4 \cdot D_i \cdot t + s_0 \tag{3.2}$$

and for confined diffusion at characteristic domain size L as

$$MSD(t) = \frac{L^2}{3} \cdot \left(1 - exp(\frac{-12 \cdot D \cdot t}{L^2})\right) + s_0 \tag{3.3}$$

In eq.(3.2) and eq.(3.3) s_0 is an offset in MSD due to the localization precision of individual proteins ($s_0 = 4\sigma^2$). Generally the MSD and α were calculated separately for each experiment. In some indicated experiments data were fit globally, with α as a free parameter and common MSDs.

3.3 Results

3.3.1 Receptor interaction is required for G-protein localization to the plasma membrane

Here we used an Ewing sarcoma-derived cells line, A673, to follow the G-protein activation upon cell-stimulation through the chemokine receptor

CXCR4. Cells were transiently transfected with either of the G-proteins, $G_{\alpha i}$-YFP, $G_{\alpha q}$-YFP including co-transfection with YFP-$G_{\beta 2}$ and $G_{\gamma 1}$ (further referred to as $G_{\beta\gamma}$-YFP) as described in Materials and Methods. It should be noted that transfection was additional to the endogenous G-protein levels present in A673 cells. Confocal imaging revealed that the expressed YFP-labeled G-proteins did not show prominent plasma membrane localization (Fig. 3.1A). The YFP-signal was predominantly found in the cytoplasm. Taken that $G_{\alpha i}$, $G_{\alpha q}$ and $G_{\beta\gamma}$ do have a membrane anchor, this suggests that the lipid anchor was not sufficient for plasma membrane localization and that specific interactions of the G-proteins with their respective GPCR-receptor was required for proper targeting. Presumably, the overexpression of G-proteins led to saturation of the endogenously expressed receptors, and, hence, affected their localization.

We tested the latter hypothesis by co-expressing G-proteins and the chemokine receptor CXCR4 such as to achieve a balanced expression of the $G_{\alpha i}$-YFP, $G_{\alpha q}$-YFP, $G_{\beta\gamma}$-YFP and the CXCR4, respectively. Since A673 cells exhibit only a low expression of endogenous CXCR4 (Sand et al., in press), co-expression led to a massive increase of CXCR4 in the cells. Since all constructs used the same promoter sequence and because we transfected with identical amounts of DNA, we assumed that similar amounts of the respective proteins were synthesized.

Confocal imaging confirmed our earlier hypothesis. Co-expression of the receptor with the G-proteins resulted in a pronounced plasma membrane localization of a fraction of both, $G_{\alpha i}$ and $G_{\alpha q}$ subunits (Fig. 3.1B). A large fraction of $G_{\alpha i}$ and $G_{\alpha q}$ stayed cytosolic (Fig. 1B). This finding corroborates earlier reports in which G_α subunits were shown to appear as both membrane-bound and cytosolic fractions (Bunemann et al., 2003). The increase in plasma membrane localization with overexpression of the receptor further suggests that a fraction of G-proteins was pre-coupled to their receptor. It is interesting to note that the localization of $G_{\beta\gamma}$ was unaltered on co-expression with CXCR4 (Fig. 3.1B). The latter finding was predicted, given that receptor/G-protein interaction is mediated by G_α but not by $G_{\beta\gamma}$ (Hamm, 2001).

Subsequently, we examined how activation of CXCR4 would affect localization of the G-proteins. We applied a continuous global stimulation with 100 nM of its specific ligand CXCL12 during time-lapse confocal imaging. At the cell perimeter no obvious change in $G_{\alpha i}$ lo-

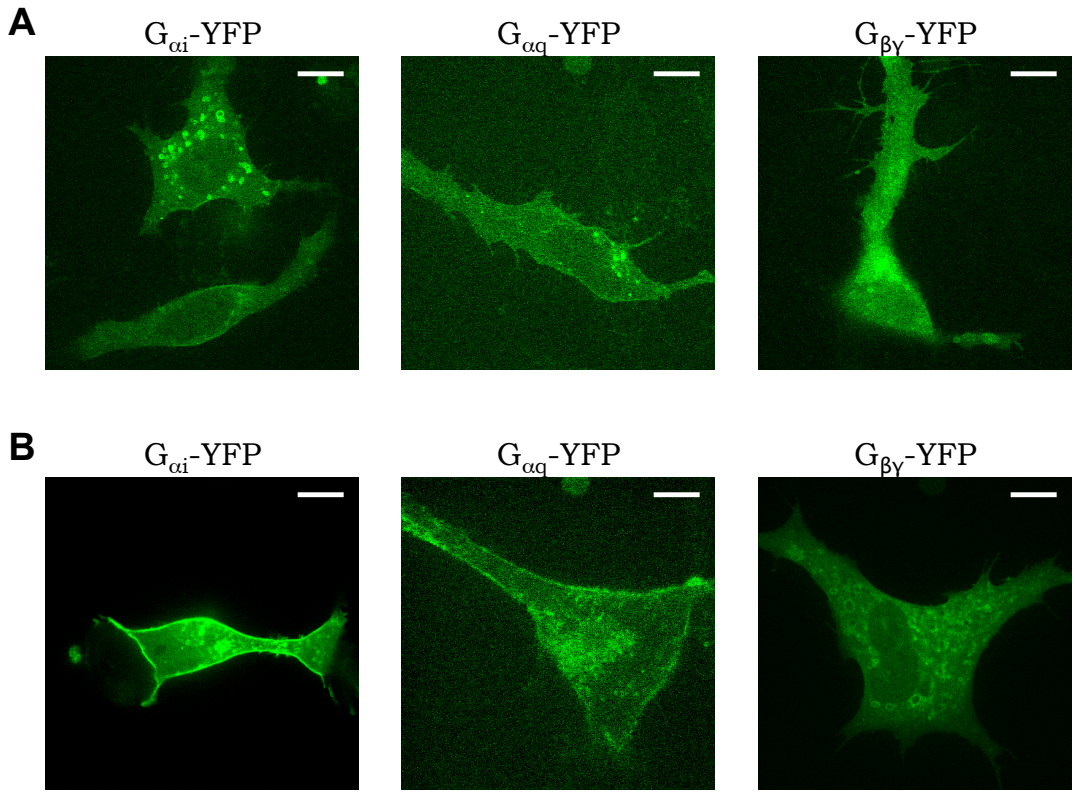

Figure 3.1
A. *A673 cells transfected with $G_{\alpha i}$-YFP, $G_{\alpha q}$-YFP or $G_{\beta\gamma}$-YFP.* ***B.*** *Co-expression of $G_{\alpha i}$-YFP, $G_{\alpha q}$-YFP or $G_{\beta\gamma}$-YFP with CXCR4. Images were acquired 24 hours after transfection. Scale bar - 10 μm.*

calization was observed. It should be noted that imaging of a specific response on a short time-scale would require a low cellular background signal, which is in contradiction with the level of $G_{\alpha i}$-YFP expression present in transfection experiments. Hence, we concentrated our further analysis to the thin membrane protrusions, which extended from the cell body (Fig. 3.2). At those locations addition of CXCL12 resulted in a prompt response of $G_{\alpha i}$ subunits. After ∼5 s of CXCL12 stimulation, $G_{\alpha i}$ exhibited a strong accumulation in small cluster-like structures seen as localized increased YFP signals (Fig. 3.2A). The clustering lasted for 20-25 s. The $G_{\alpha q}$ subunit showed a similar accumulation in cluster-like structures with the same dynamic behavior (Fig. 3.2B). Both for $G_{\alpha i}$ and $G_{\alpha q}$ clustering did not re-occur for at least the following 30 minutes (length of the experiment; data not shown). Thus, $G_{\alpha i}$ and $G_{\alpha q}$

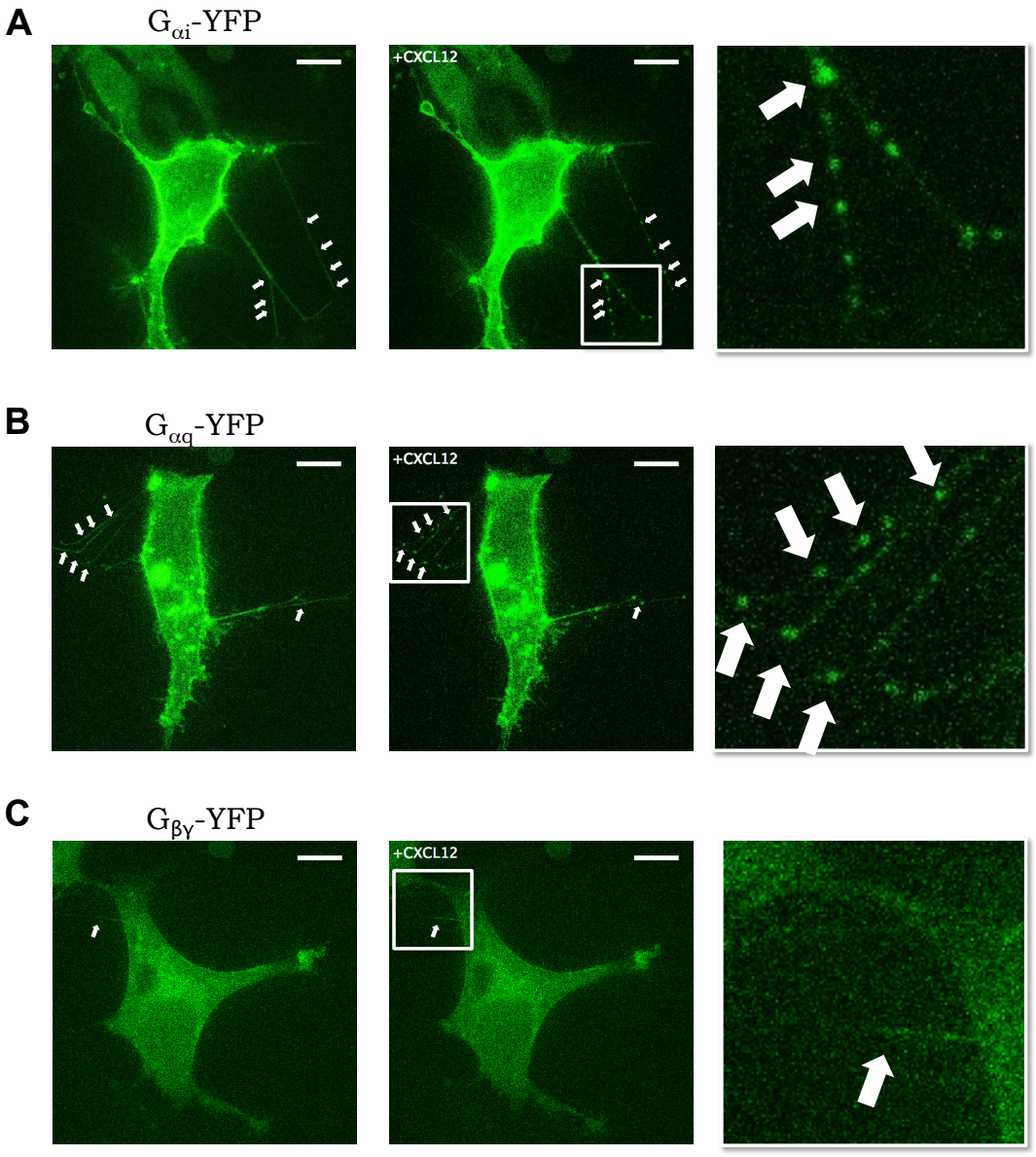

Figure 3.2
*A673 cells co-expressing of $G_{\alpha i}$-YFP **(A)**, $G_{\alpha q}$-YFP **(B)** or $G_{\beta\gamma}$-YFP **(C)** with CXCR4 before (left) and during (middle and right) global stimulation of CXCR4 with 100 nM of CXCL12. Scale bar - 10 μm.*

subunits exhibit a fast short-term response upon CXCR4 receptor activation. CXCL12 stimulation did not display a similar effect on the $G_{\beta\gamma}$ subunits during the first seconds of incubation with the ligand (Fig. 3.2C).

In summary, the results showed that activation of CXCR4 is followed by a re-localization of the plasma membrane-bound fraction of G-proteins. Given that the response was fast, on the timescale of seconds, we in turn hypothesized that a fraction of the G proteins potentially was pre-coupled to the receptor in order to allow for the fast response observed.

3.3.2 Mobility of membrane proteins is unaltered on cell-substrate adhesion

To obtain a deeper insight into the behavior of the membrane-anchored fraction of G-proteins and learn about the dynamic behavior after cell stimulation we applied single-molecule fluorescence microscopy. Inasmuch as G-proteins were present in two fractions, a cytoplasmic and a membrane-anchored fraction, single-molecule experiments required restriction of our analysis to the thin (least cytoplasm-containing) parts of the cell. In this configuration it is experimentally difficult to distinguish top and bottom membrane of a cell during the single-molecule imaging. Thus, we used a well-studied control system, CXCR4-YFP in A673 cells (Chapter 2 of this thesis), to elicit whether membrane interaction with the surface of the dish would affect the motility of membrane-associated molecules.

Similar to our previous study (Chapter 2 of this thesis), we accessed the diffusion dynamics of individual CXCR4-YFP on the millisecond time-scale as described in Materials and Methods. We detected individual CXCR4-YFP with ∼40 nm localization precision and determined their mobility on the proximal (bottom) and the distal (top) plasma membrane.

As reported earlier two fractions of different mobility were observed, in which one was mobile and the other immobile. The fraction size α, and mean square displacements (MSD) were determined subsequently. Our results showed that the MSD was indistinguishable between the top (filled black and red circles) and the bottom (open black and red circles) membrane when observed for time-lags between 50 and 250 ms (Fig. 3.3A).

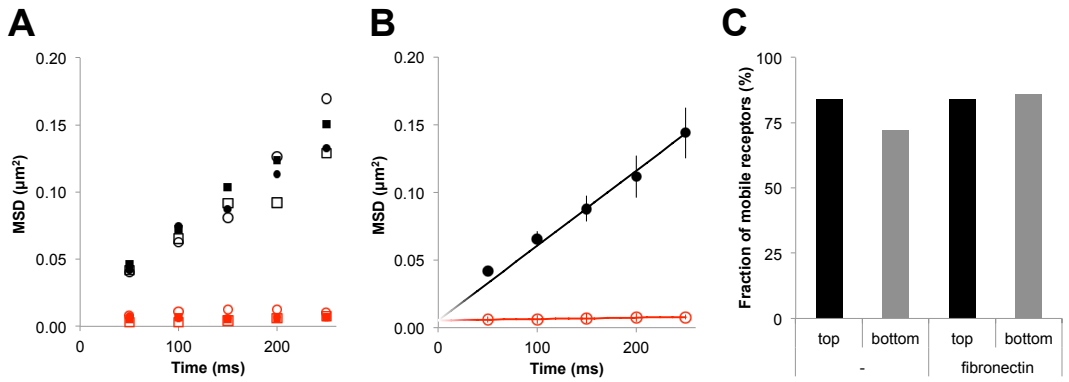

Figure 3.3
Comparison of CXCR4 mobility at top and bottom part of the plasma membrane. ***A.*** *Mean square displacement of mobile (black) and immobile (red) receptors determined at the top (filled symbols) and bottom (open symbols) membrane of cells placed on plastic dishes (circles) or on dishes pre-coated with fibronectin (squares).* ***B.*** *Change of mean square displacement (MSD) with time for mobile (black circles) and immobile (red open circles) receptors. Data were fit to a free diffusion model (black and red lines).* ***C.*** *Comparison of the fractions of mobile receptors detected at the top (black) and bottom (grey) membrane for cells placed on non-treated or fibronectin pre-coated dishes.*

The linear dependence of the mean squared displacement with time lag confirmed that the mobility for the mobile fraction was described by free diffusion, characterized by a diffusion coefficient of $D_{CXCR4} = 0.14 \pm 0.01\ \mu m^2/s$ (Fig. 3.3B). The fraction size of the mobile receptors on top and bottom membranes was identical within error and yielded ~80% (Fig. 3.3C). All values were in excellent agreement with the values reported earlier by us for the distal membrane (Chapter 2 of this thesis).

We further examined whether enhanced cell adhesion would affect diffusion of the receptors. A673-CXCR4 cells were placed on dishes that were pre-coated with fibronectin. Interaction of the cells with fibronectin did not alter the mobility of CXCR4 (Fig. 3.3). Both the diffusion coefficient (Fig. 3.3A,B) and the size of the mobile fraction (Fig. 3.3C) resembled those of the control.

Our results demonstrate that membrane interaction with the surface of the dish did not alter the diffusion dynamics of the trans-membrane chemokine receptor CXCR4. Hence, it is conceivable that the mobility of G-proteins, which are only membrane-bound to the inner plasma membrane leaflet, would be likewise undisturbed. This finding largely

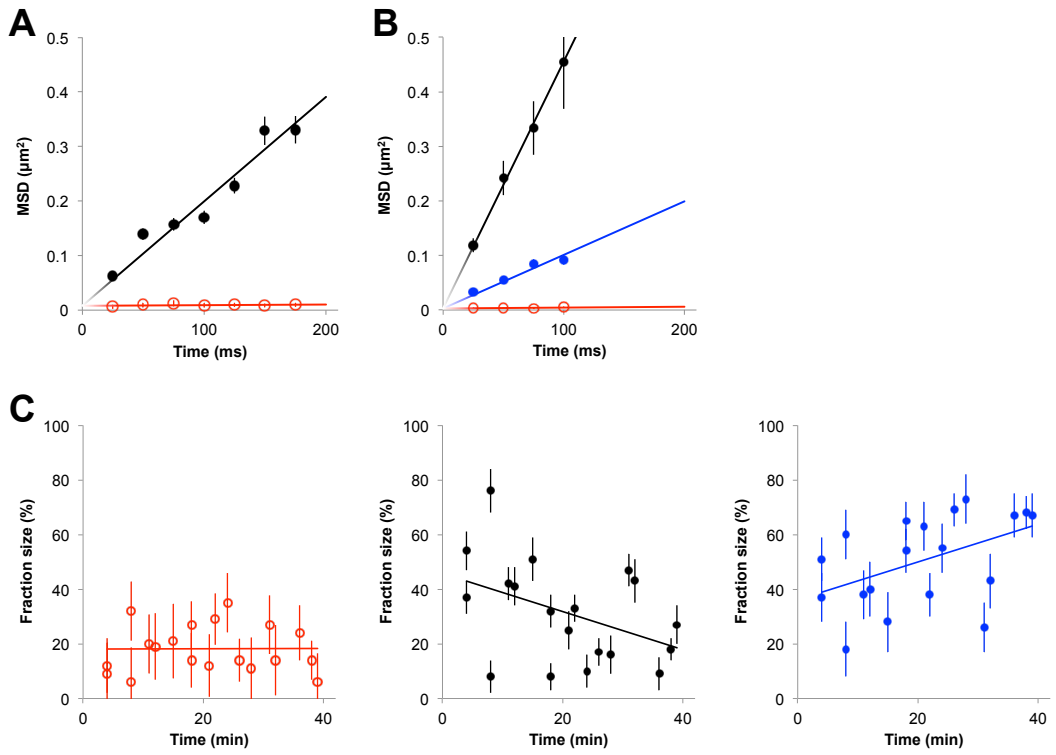

Figure 3.4
Mobility of $G_{\alpha i}$. ***A.*** *MSD vs. time determined for fast diffusing (black) and immobile (red) $G_{\alpha i}$ molecules in resting A673 cells.* ***B.*** *MSD of fast diffusing (black), slow diffusing (blue) and immobile (red) molecules for cells stimulated by 100 nM of CXCL12. The data were globally fitted to a 3-fraction diffusion model. Solid lines represent the respective fit of the data.* ***C.*** *Time-dependent change of the fraction sizes of immobile (open red) and fast (black) and slow (blue) diffusing $G_{\alpha i}$ molecules during continuous stimulation of CXCR4 with 100 nM CXCL12.*

simplified further experiments since it did not require the distinction of the top and bottom membrane in the analysis.

3.3.3 Binding of $G_{\alpha i}$ to CXCR4 requires receptor activation

Single-molecule imaging was used to study the mobility of individual membrane-bound G-protein subunits. As anchoring of G-proteins to the plasma membrane is facilitated through a membrane-binding lipid moiety, which is much smaller compared to the size of the CXCR4 receptor, one can predict that receptor-decoupled G-proteins were characterized

by a significantly increased diffusion constant in relation to GPCR-bound G-proteins.

In resting cells the $G_{\alpha i}$-subunits existed in two fractions, a mobile and an immobile fraction (Fig. 3.4A). The mobile fraction of 76±2%, followed free diffusion characterized by a diffusion coefficient of $D_{G\alpha i} = 0.48\pm0.02\ \mu m^2/s$. This value was significantly higher than that of the CXCR4 receptor ($D_{CXCR4} = 0.14 \pm 0.01\ \mu m^2/s$). Thus, our results confirmed the prediction made above. For resting cells there was no detectable fraction of $G_{\alpha i}$ that would exhibit a diffusion behavior similar to the mobile fraction of the CXCR4. This observation leads to the conjecture that the mobile fractions of $G_{\alpha i}$ and CXCR4 were not coupled prior to CXCL12 stimulation.

Next we applied 100 nM of CXCL12 to specifically activate CXCR4 and subsequently monitored changes in the mobility of $G_{\alpha i}$. Our results revealed, that there was no significant change in the size of the immobile fraction of $G_{\alpha i}$, compared to that before stimulation (18±9 % and 24±2 %, respectively). Taken our earlier finding that the fraction of immobile CXCR4 increased upon activation, this result suggested that the immobile fraction of the $G_{\alpha i}$ was also independent and not coupled to the immobile receptors (Chapter 2 of this thesis). Further we found that the mobile fraction of the $G_{\alpha i}$-subunits was split into two diffusive fractions, a fast and a slow fraction (Fig. 3.4B) with diffusion coefficients $D_{G\alpha i(fast)} = 1.13\pm0.02\ \mu m^2/s$ and $D_{G\alpha i(slow)} = 0.25\pm0.01\ \mu m^2/s$, respectively. The diffusion coefficient of the slow fraction was comparable to that of the mobile CXCR4 receptor. This finding implies that CXCL12 stimulation lead to a physical interaction of $G_{\alpha i}$ and CXCR4, which lasted at least for 150 ms, the longest time-lag we investigated.

We next followed the value of the mobile fractions of $G_{\alpha i}$ after continued stimulation with CXCL12 for 30 minutes. On this time scale the size of the fast fraction (Fig. 3.4C, middle) exhibited a tendency to decrease at a rate of $\sim 1\% min^{-1}$. Interestingly, we observed the appearance of the slow fraction of $G_{\alpha i}$ within the first minutes after CXCL12 addition exhibiting a tendency to increase at the same rate. This result is in excellent agreement with earlier findings by FRET that showed the onset of $G_{\alpha i}$/receptor coupling on time scale of seconds (Bunemann et al., 2003).

Thus, our data showed that interaction of $G_{\alpha i}$ with CXCR4 is dependent on and occurs after receptor stimulation, suggesting that $G_{\alpha i}$/

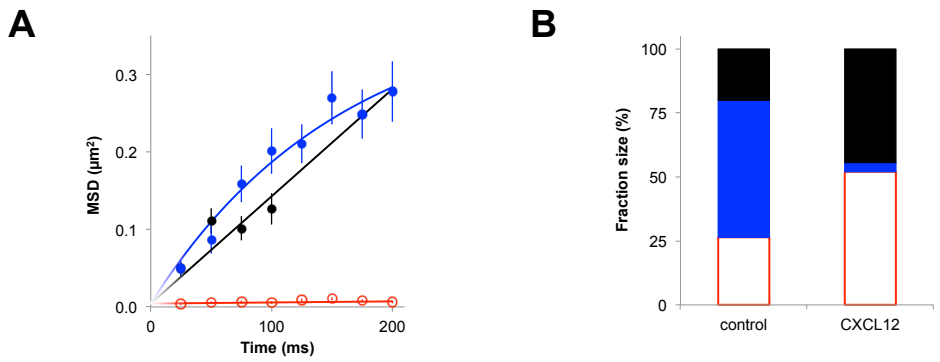

Figure 3.5
Mobility of $G_{\alpha q}$. ***A.*** *Mean square displacement (MSD) of fast diffusing (black), confined (blue) and immobile (red) molecules as resulting from a global fit of the resting and CXCL12 stimulated cells. Solid lines represent the respective fit of the data. The linear size of the confinement zone yielded $L = 1.1 \pm 0.1$ µm.* ***B.*** *Comparison of fraction sizes of fast diffusing (black), confined (blue) and immobile (open red) $G_{\alpha q}$ molecules in resting cells or upon CXCR4 activation with 100 nM CXCL12.*

CXCR4 follows a 'collision coupling' model described earlier (Hein and Bunemann, 2008).

3.3.4 $G_{\alpha q}$ is pre-coupled to an inactive CXCR4 receptor

Next we addressed the mobility of individual $G_{\alpha q}$ subunits. Similar to the $G_{\alpha i}$ subunits, $G_{\alpha q}$ existed in mobile and immobile states in resting cells. However, already before activation of the receptor, the mobile fraction of the $G_{\alpha q}$-subunits was split into 2 populations (Fig. 3.5), a fast fraction characterized by $D_{G\alpha q(fast)} = 0.35 \pm 0.04$ µm^2/s and a slow fraction characterized by $D_{G\alpha q(slow)} = 0.15 \pm 0.02$ µm^2/s. To our surprise, the fraction of slow $G_{\alpha q}$ molecules (54±11%) was the dominant fraction (Fig. 3.5B). Activation of CXCR4 by 100 nM CXCL12 resulted in a drastic change in $G_{\alpha q}$ fraction sizes (Fig. 3.5B). The fast fraction increased to 44±5% compared to resting cells (20±14%), while the slow fraction dropped to 4±3% when compared to the resting state (54±11%). Moreover, the fraction of immobile $G_{\alpha q}$-subunits increased from 26±18% in resting cells to 52±6% in cells with activated CXCR4 receptors (Fig. 3.5B).

These results suggest that, in contrast to the $G_{\alpha i}$ subunit, $G_{\alpha q}$ ap-

peared to be pre-coupled to the CXCR4 receptor in resting cells. Upon receptor activation $G_{\alpha q}$ subunits either uncouple from CXCR4, as reflected in an increase of the fast fraction, or are immobilized. Earlier we reported a likewise immobilization of CXCR4 upon stimulation that was related to receptor internalization (Chapter 2 of this thesis), suggesting that the immobilized $G_{\alpha q}$ fraction might be associated to a receptor/G-protein complex destined to internalization.

3.4 Discussion

Signalling by the chemokine receptor CXCR4 is a complex process which includes activation of G-protein dependent and independent pathways ultimately regulating gene expression, cell proliferation, survival, and chemotaxis (Teicher and Fricker, 2010). The ensemble of G-protein dependent pathways activated by CXCR4 involves signalling through four various G_{α} subunits (Rubin, 2008). Thus, the orchestration of all the signalling cascades in time and space has to be tightly controlled. Here we investigated the mechanism of CXCR4 interaction with G-proteins and its relation to the receptor signalling. Our data suggested a sequential receptor binding of $G_{\alpha q}$ and $G_{\alpha i}$, which would result in a temporal ordering of the signalling (Fig. 3.6).

In the inactive state CXCR4 appeared to be coupled to the $G_{\alpha q}$ subunit. This conclusion followed from the detected fraction of $G_{\alpha q}$ that displayed an identical mobility when compared to the mobility of the inactive CXCR4. Furthermore, the respective fraction was lost after receptor activation by CXCL12, implying uncoupling of $G_{\alpha q}$ from the receptor after activation. It is known that $G_{\alpha q}$ activation leads to a Ca^{2+} influx through the phospholipase-Cβ (PLCβ) pathway (Rubin, 2008). The Ca^{2+} influx is fast, observable from the first moments after receptor activation (Fig. 3.6), indicating immediate triggering of the PLCβ cascade, thus, further supporting our assumption of pre-coupling of $G_{\alpha q}$ to CXCR4.

The release of $G_{\alpha q}$-subunit from the stimulated receptor subsequently allows coupling of the $G_{\alpha i}$-subunit to CXCR4 with concomitant activation of $G_{\alpha i}$. This conclusion followed from our mobility analysis, which suggested that in the inactive state CXCR4 was not coupled with $G_{\alpha i}$. Upon CXCR4 stimulation with CXCL12 a receptor-bound fraction of $G_{\alpha i}$ was observed. This receptor-bound fraction of $G_{\alpha i}$ increased with

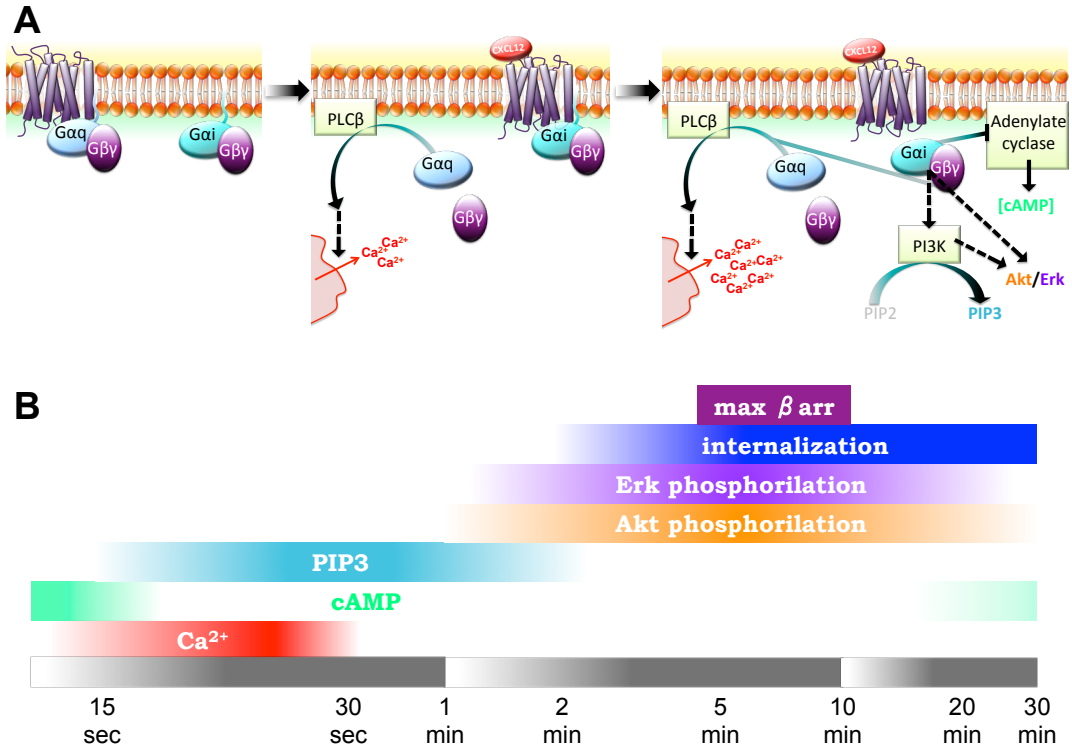

Figure 3.6

Schematic representation of the CXCR4 signalling sequence. ***A.*** *Model of sequential activation of the G-proteins and respective pathways.* ***B.*** *The time-line (in log scale) of CXCR4 signalling after CXCL12 stimulation. The slow increase and fast decrease of Ca^{2+} flux is detected from the first moments and lasts for ∼20-30 seconds (Arnolds et al., 2013; Busillo et al., 2010; Mueller et al., 2013; Sotsios et al., 1999; Tripathi et al., 2014). A decrease of cAMP concentration is delayed and has a prolongated effect of ∼30 minutes (Yang et al., 2007). Between ∼15 seconds and 2 minutes after receptor activation, an elevated concentration of PIP3 is detected (Sotsios et al., 1999). A maximum of Akt and Erk phosphorylation is attained 5-10 minutes after stimulation (Brennecke et al., 2014; Kawaguchi et al., 2009; Sotsios et al., 1999; Torossian et al., 2014; Wojcechowskyj et al., 2011; Zhao et al., 2006). G-protein independent receptor internalization is detected as soon as 2 minutes after addition of the ligand (Busillo et al., 2010; Mueller et al., 2013; Tripathi et al., 2014; Venkatesan, 2003). A maximum of β-arrestin recruitment appears at 5-10 minutes (Busillo et al., 2010).*

time, suggesting a prolonged activation of $G_{\alpha i}$. It is known that $G_{\alpha i}$ activation results in a decrease of intracellular cyclic AMP (cAMP) concentration through the adenylate cyclase inhibition (Fig. 3.6). This decrease has been observed with a delay after receptor activation and has been reported as long lasting (Fig. 3.6) (Yang et al., 2007). Those earlier biochemical findings were corroborated by our findings based on protein mobility showing a delayed and prolonged $G_{\alpha i}$/CXCR4 coupling.

It is interesting to note that $G_{\alpha q}$ and $G_{\alpha i}$ subunits were shown cross-activate intracellular signalling pathways. Activation of $G_{\alpha q/11}$-coupled receptors was shown to be crucial for signalling by various $G_{\alpha i/o}$-coupled receptors (Bakker et al., 2004). For instance, $G_{\alpha q}$-stimulated PLCβ-activity was increased by $G_{\alpha i}$-linked receptors (Chan et al., 2000). Hence, the sequential activation of $G_{\alpha q}$ and $G_{\alpha i}$ by CXCR4 could be a mechanism to control the activation of specific pathways. One potential scenario would be that receptor activation causes an immediate activation of the pre-coupled $G_{\alpha q}$ and, thus, of PLCβ followed by $G_{\alpha q}$ uncoupling. The sequential and prolonged interaction of CXCR4 with $G_{\alpha i}$, in turn would further promote PLCβ signalling. Inasmuch as the PLCβ-pathway is associated with the chemotactic response (Teicher and Fricker, 2010) such a signalling control and amplification mechanism might be involved in the initial steps of the gradient sensing.

In summary, our results showed that the chemokine receptor CXCR4 has a differential coupling with various G_{α}-subunits. The coupling with $G_{\alpha q}$ corresponds to 'pre-coupled' model, while coupling with $G_{\alpha i}$ follows 'collision coupling' model. Such difference in the coupling appears to be a mechanism of controlling the subsequent activation of respective pathways and, thus, an important mechanism to specific CXCR4 signal transduction.

3.5 Acknowlegement

We would like to thank the Bunemann Lab, who generously shared the G-protein containing plasmids. We would like to thank Sylvie Olthuis for preparation of the described clones of the plasmids.

3.6 References

Arnolds, K., Lares, A., and Spencer, J. (2013). The US27 gene product of human cytomegalovirus enhances signalling of host chemokine receptor CXCR4. Virology.

Bakker, R., Casarosa, P., Timmerman, H., Smit, M., and Leurs, R. (2004). Constitutively active Gq/11-coupled Receptors Enable Signaling by Co-expressed Gi/o-coupled Receptors. Journal of Biological Chemistry.

Brennecke, P., Arlt, M., Campanile, C., Husmann, K., Gvozdenovic, A., Apuzzo, T., Thelen, M., Born, W., and Fuchs, B. (2014). CXCR4 antibody treatment suppresses metastatic spread to the lung of intratibial human osteosarcoma xenografts in mice. Clin Exp Metastasis.

Bunemann, M., Frank, M., and Lohse, M.J. (2003). Gi protein activation in intact cells involves subunit rearrangement rather than dissociation. Proc. Natl. Acad. Sci. U.S.A. 100, 16077-16082.

Busillo, JM, Armando, S, Sengupta, R, and Meucci, O (2010). Site-specific phosphorylation of CXCR4 is dynamically regulated by multiple kinases and results in differential modulation of CXCR4 signaling. Journal of Biological

Chan, J.S., Lee, J.W., Ho, M.K., and Wong, Y.H. (2000). Preactivation permits subsequent stimulation of phospholipase C by G(i)-coupled receptors. Mol. Pharmacol. 57, 700-708.

Fredriksson, R., Lagerstrom, M.C., Lundin, L.-G.G., and Schioth, H.B. (2003). The G-protein-coupled receptors in the human genome form five main families. Phylogenetic analysis, paralogon groups, and fingerprints. Mol. Pharmacol. 63, 1256-1272.

Hamm, H. (2001). How activated receptors couple to G proteins. Proceedings of the National Academy of Sciences.

Hein, P., and Bunemann, M. (2008). Coupling mode of receptors and G proteins. Naunyn-Schmied Arch Pharmacol.

Hein, P., Frank, M., Hoffmann, C., Lohse, M.J., and Bunemann, M. (2005). Dynamics of receptor/G protein coupling in living cells. EMBO J. 24, 4106-4114.

Van Hemert, F., Lazova, M.D., Snaar-Jagaska, B.E., and Schmidt, T. (2010). Mobility of G proteins is heterogeneous and polarized during chemotaxis. J. Cell. Sci. 123, 2922-2930.

Van Hoorn, H., Harkes, R., Spiesz, E.M., Storm, C., van Noort, D., Ladoux, B., and Schmidt, T. (2014). The nanoscale architecture of

force-bearing focal adhesions. Nano Lett. 14, 4257-4262.

Kawaguchi, A., Orba, Y., Kimura, T., Iha, H., Ogata, M., Tsuji, T., Ainai, A., Sata, T., Okamoto, T., Hall, W.W., et al. (2009). Inhibition of the SDF-1alpha-CXCR4 axis by the CXCR4 antagonist AMD3100 suppresses the migration of cultured cells from ATL patients and murine lymphoblastoid cells from HTLV-I Tax transgenic mice. Blood 114, 2961-2968.

Lohse, M.J., Hein, P., Hoffmann, C., Nikolaev, V.O., Vilardaga, J.-P.P., and Bunemann, M. (2008). Kinetics of G-protein-coupled receptor signals in intact cells. Br. J. Pharmacol. 153 Suppl 1, S125-32.

Milligan, G., and Kostenis, E. (2006). Heterotrimeric G-proteins: a short history. British Journal of Pharmacology.

Mueller, W, Schutz, D, Nagel, F, Schulz, S, and Stumm, R (2013). Hierarchical organization of multi-site phosphorylation at the CXCR4 C terminus.

Qin, K., Sethi, P.R., and Lambert, N.A. (2008). Abundance and stability of complexes containing inactive G protein-coupled receptors and G proteins. FASEB J. 22, 2920-2927.

Rubin, J. (2008). Chemokine signaling in cancer: one hump or two? Semin. Cancer Biol.

Schmidt, T, Schutz, GJ, and Baumgartner, W (1996). Imaging of single molecule diffusion. Proceedings of the

Semrau, S, and Schmidt, T (2007). Particle image correlation spectroscopy (PICS): retrieving nanometer-scale correlations from high-density single-molecule position data. Biophysical Journal.

Sotsios, Y., Whittaker, G.C., Westwick, J., and Ward, S.G. (1999). The CXC chemokine stromal cell-derived factor activates a Gi-coupled phosphoinositide 3-kinase in T lymphocytes. The Journal of Immunology 163, 5954-5963.

Teicher, and Fricker (2010). CXCL12 (SDF-1)/CXCR4 Pathway in Cancer. Clinical Cancer Research.

Torossian, F., Anginot, A., Chabanon, A., Clay, D., Guerton, B., Desterke, C., Boutin, L., Marullo, S., Scott, M.G., Lataillade, J.-J.J., et al. (2014). CXCR7 participates in CXCL12-induced CD34+ cell cycling through β-arrestin-dependent Akt activation. Blood 123, 191-202.

Tripathi, A., Davis, J.D., Staren, D.M., Volkman, B.F., and Majetschak, M. (2014). CXC chemokine receptor 4 signaling upon co-activation with stromal cell-derived factor-1α and ubiquitin. Cytokine

65, 121-125.

Venkatesan (2003). Distinct Mechanisms of Agonist-induced Endocytosis for Human Chemokine Receptors CCR5 and CXCR4. Molecular Biology of the Cell.

Wojcechowskyj, J.A., Lee, J.Y., Seeholzer, S.H., and Doms, R.W. (2011). Quantitative phosphoproteomics of CXCL12 (SDF-1) signaling. PLoS ONE 6, e24918.

Yang, L., Jackson, E., Woerner, M., Perry, A., Piwnica-Worms, D., and Rubin, J. (2007). Blocking CXCR4-Mediated Cyclic AMP Suppression Inhibits Brain Tumor Growth In vivo. Cancer Research.

Zhao, M, DiScipio, RG, and Wimmer, AG (2006). Regulation of CXCR4-mediated nuclear translocation of extracellular signal-related kinases 1 and 2. Molecular Pharmacology.